Toward "S"-Shaped 3D-Printed Soft Robotic Guidewires for Pediatric Patent Ductus Arteriosus Endovascular Interventions

Adira Colton[1], Declan Fitzgerald[1], Sunandita Sarker[1], Noah Barnes[2], Dheeraj Gandhi[3], Miroslaw Janowski[3], Jeremy D. Brown[2], Joshua Kanter[4], Laura Olivieri[5], Mark Fuge[1,6], Axel Krieger[2], and Ryan D. Sochol[1,6,7]

***Abstract*—Patent Ductus Arteriosus (PDA) is a heart condition in which the ductus arteriosus—a blood vessel connecting the pulmonary artery to the aorta in a fetus—fails to undergo closure after birth. A PDA can be an important factor in neonates born with severe congenital heart disease (CHD) or born prematurely. With the advent of new intravascular stent technologies, treatments based on ductus arteriosus stenting can now be completed in many cases; however, difficulties remain in accessing the ductus arteriosus in small babies successfully using current guidewire-catheter systems. Recent developments for soft robotic endovascular instruments that leverage control schemes hold distinctive potential for addressing these access challenges, but such technologies are not yet at the sizes required for navigating neonatal vasculature safely and efficiently. In an effort to meet this clinical need, this work presents an approach for 3D printing 1.5 French (Fr) soft robotic guidewires that transition from straight to "S"-shaped configurations under the application of fluidic (*e.g.*, pneumatic or hydraulic) loading. Two distinct dual-opposing segmented soft actuators, including a symmetric and asymmetric system design (both with heights of 2.5 mm), were 3D printed onto 1.1 Fr capillaries in 35–60 minutes *via* "Two-Photon Direct Laser Writing (DLW)". Experimental results revealed that both designs not only withstood pressures of up to 550 kPa, but also exhibited increased opposing bending deformations—corresponding to decreased radii of curvature—with increasing applied pressure. In combination, this study serves as a critical foundation for next-generation fluidically actuated soft robotic guidewire-catheter systems for PDA interventions.**

This work was supported in part by U.S. National Institutes of Health Award Number 1R01EB033354 and U.S. National Science Foundation Award Number 1943356. This work was also supported in part by the Maryland Robotics Center and the Center for Engineering Concepts Development at the University of Maryland. This material is based upon work supported by the National Science Foundation Graduate Research Fellowship Program under Grant No. DGE2236417 and DGE2139757.

[1]Department of Mechanical Engineering, University of Maryland, College Park, MD, 20742, USA. Email: {acolton1, dfitzge2, ssarker1, fuge, rsochol} @umd.edu

[2]Department of Mechanical Engineering, Johns Hopkins University, Baltimore, MD, 21218, USA. Email: {nbarne18, jdelainebrown, axel}@jhu.edu

[3]Program in Image Guided Neurointerventions, Department of Diagnostic Radiology and Nuclear Medicine, University of Maryland School of Medicine, Baltimore, MD, 21201, USA. Email: dgandhi@umm.edu, miroslaw.janowski @som.umaryland.edu

[4]Children's National Heart Institute, Children's National Hospital, Washington DC, 20010, USA. Email: jkanter@childrensnational.org

[5]Department of Pediatrics, University of Pittsburgh School of Medicine, Pittsburgh, PA 15224, USA. Email: olivierilj@upmc.edu

[6]Maryland Robotics Center, University of Maryland, College Park, MD, 20742, USA.

[7]Robert E. Fischell Institute for Biomedical Devices, University of Maryland, College Park, MD, 20742, USA.

I. Introduction

A. Patent Ductus Arteriosus

A patent ductus arteriosus (PDA) can be an important factor in two specific groups of neonates. First, some infants born with severe congenital heart disease (CHD) do not have enough pulmonary blood flow and therefore require an extra connection to the pulmonary arteries for adequate blood flow to the lungs [1]. Other infants with severe CHD have the opposite problem, wherein there is not enough systemic blood flow and an extra connection to the aorta is required [2], [3]. Traditionally, this extra connection (or shunt) was placed *via* heart surgery in the neonatal period for both groups of infants. With the advent of new intravascular stent technology, however, ductus arteriosus stenting can now be successfully completed for a variety of severe congenital heart defects to create the extra connection needed for either systemic or pulmonary blood flow. The ductal stenting procedure delays the need for surgical correction and allow babies to grow larger and stronger in the interim. Early and mid-term results of ductal stenting are outstanding, with lower length of stay, better growth, and better operative outcomes [4], [5]. Unfortunately, not every infant who could benefit from this procedure is able to do so, in part due to difficulties associated with accessing the ductus arteriosus [6], [7]. The path between the catheter access point and the ductus arteriosus can sometimes involve tortuous and complex curvature, which is difficult to achieve in small babies with current guidewire-catheter technologies [8], [9].

The second group involves infants born prematurely who are at risk of development of a PDA, which increases risk of morbidity and mortality, and because it rarely undergoes spontaneous closure, closure *via* surgery is often required [10]. Prematurity is prevalent throughout the US, with rates increasing over the past 50 years. The presence of a PDA—which is highly associated with prematurity—significantly affects the hemodynamic and cardiopulmonary stability of infants' receiving care in the neonatal ICU [11]. Unlike the infants with CHD that benefit from maintaining the PDA, premature infants with no CHD can be injured substantially by the presence of their PDAs, and so these babies benefit from PDA closure. Until the recent development of US FDA-approved miniature intravascular devices for use to occlude a PDA in babies who weigh 550 g or more, PDAs in premature babies were surgically ligated *via* open heart surgery with a

left thoracotomy approach, which has yielded dramatic improvements in post-PDA closure care and avoided invasive surgeries in thousands of babies [12-14]. Yet, not every baby who could benefit from PDA device closure is able to, in part due to the same difficulty accessing the ductus arteriosus through tiny blood vessels [15]. Thus, there is a current unmet clinical need for improved catheters that are able to safely and efficiently navigate tight, significant turns in small babies to allow for lifesaving interventional procedures, including PDA stenting in severe CHD as well as PDA closure in prematurity.

B. Soft Robotics for Endovascular Interventions

The field of soft robotics is uniquely suited to the development of medical robotics due to their inherent flexibility, which can reduce trauma and increase safety when compared to traditional robotics [16-18]. Specifically, for catheterization interventions, soft robots can address the navigational challenges posed by complex human vasculature by allowing the interventionalist to actively control the direction of travel for the tool and to deliver treatment to the most hard-to-reach locations [19], [20]. The anatomy of the human heart specifically offers a challenge to interventionalists given its tortuous vasculature [21], and many soft robotic catheters have been developed to address this gap [22], [23]. These catheters were designed for adult hearts, however, and cannot be used in the small vasculature of an infant with PDA.

A large limiting factor in the development of soft robotic surgical catheters and guidewires is the size scales in which certain manufacturing strategies are limited. For larger catheterization surgeries such as urethral and endoscopy, that limiting factor plays less of a role [24-27]. Additive manufacturing (or "3D printing") allows for complex geometries not manufacturable with traditional manufacturing, including for macroscale soft robotic actuators [28], [29]. For microscale soft robots, however, "Two-Photon Direct Laser Writing (DLW)" is uniquely suitable.

Previously, our group has developed DLW-printed 3D microscale soft robotic actuators [30], [31] as well as a strategy termed "*ex situ* Direct Laser Writing (esDLW)", which allows for DLW-based printing directly on top of (and fluidically sealed to) macroscale fluidic tubing [31-33]. To address the challenges in pediatric PDA surgical tools, here we present two dual-opposing segmented soft robotic guidewire heads printed atop fused silica tubing *via es*DLW (Fig. 1a). In this work, we present both a symmetric and an asymmetric design (Fig. 1b). The segments of the robots are connected such that from a single pressure input, the bottom segment and the top segment actuate in opposing directions (Fig. 1b) to create the 'S' shape necessary to navigate through an infant's cardiovasculature to the location of the PDA (Fig. 1c).

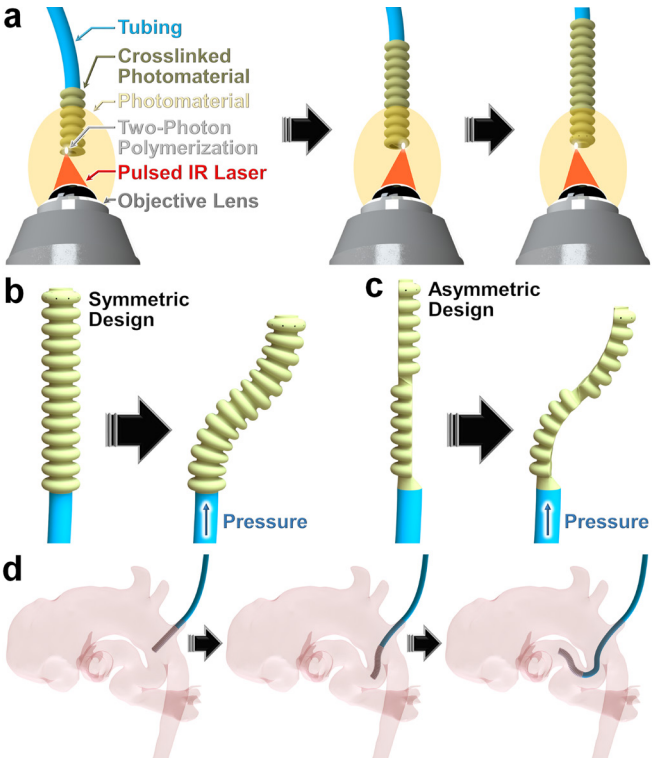

Figure 1. Conceptual illustrations of the manufacturing strategy for 3D microprinting integrated soft actuators directly atop—and fluidically sealed to—medical tubing as a means to fabricate fluidically actuated soft microrobotic surgical tools. (a) The "*ex situ* Direct Laser Writing (*es*DLW)" process for 3D microprinting integrated soft actuators onto fused silica capillary tubing *via* two-photon polymerization. (b) The symmetric design with no pressure input and then under an applied pressure input, in which the "S" shape becomes more defined with larger pressures. (c) The asymmetric design, with similar pressure-based actuation. (d) An example of how the guidewire would traverse through an infant's vasculature *via* a left subclavian approach to reach the patent ductus arteriosus (3D render of heart vasculature courtesy of Children's National Hospital, Washington, DC).

II. Materials and Methods

A. Ex Situ Direct Laser Writing (esDLW) Fabrication

The soft robotic guidewire heads were manufactured *via* our *es*DLW methodology [31-33]. First, the guidewire heads were modeled using SolidWorks (Dassault Systems, France) computer-aided design (CAD) software and exported as an STL file. The bellows were designed with a wall thickness of 20 μm, which enables actuation while allowing for the actuator to support its own weight. The files were imported into DeScribe (Nanoscribe, Karlsruhe, Germany) computer-aided manufacturing (CAM) software to generate the point-by-point, layer-by-layer writing paths for the laser.

Before starting the print, fused silica polyimide-coated capillaries (Molex LLC, Lisle, IL) with an inner diameter of 75 μm and an outer diameter of 360 μm were cut using a Shortix Capillary Cutter (Postnova Analytics Inc, Salt Lake City, UT), which contains a diamond cutting blade to ensure a clean cut and smooth surface for printing. The capillaries were rinsed successively with acetone and isopropyl alcohol (IPA) and then dried with N_2 gas, then loaded into a Plasma Cleaner (Pie Scientific, Union City, CA) at 75 watts for 30 min. Immediately after removal from the plasma cleaner, the capillary tubes were submerged in a prepared silane solution of 0.5% v/v 3-(trimethoxysilyl)propyl methacrylate in ethanol for at least 30 min. This silanization process was performed to increase adhesion between the fused silica surface and the

resin used in the print. Finally, the capillaries were rinsed with acetone and water, and then dried with N_2 gas.

The fully prepared capillaries were then loaded into a Nanoscribe Photonic Professional GT2 DLW 3D printer in a custom-made holder. The photoresin, IP-Dip2 (Nanoscribe), was deposited onto the 10× lens such that the droplet covered the glass cover on the objective. This precise volume of deposited resin allows enough resin for taller prints, but also prevents the resin meniscus from breaking and the resin flowing away from the print. The resin was also injected back into the capillary from the printing surface to prevent air bubbles from exiting the center of the tube mid-print. The polyimide coating on the tubing burns if the IR laser interacts with it, so the outer diameter of the base of the guidewire head was designed to be smaller than that of the capillary tube. The interface of the capillary was found manually and the print was started with roughly 45 μm of overlap with the capillary to fill any unevenness in the capillary surface. The print was run with 100% laser power and a scan speed of 30,000 μm/s.

The prints were developed inverted vertically inside of propylene glycol monomethyl ether acetate (PGMEA) on a hot plate heated to 35 °C for 1 hr, with fresh PGMEA swapped in after 30 min. To aid this development stage, 22 μm clearing holes were included at the top of the actuators to allow diffusion of PGMEA into the bellows (but were small enough to prevent an impact on subsequent actuation). During this stage, suction was pulled back through the print, drawing PGMEA into the guidewire head *via* the clearing holes built into the top bellow of the design. The prints were then soaked in IPA overnight (~12 hrs).

B. Experimental Set-Up

The opposing ends of the fused silica capillaries with the guidewire head printed on top were inserted into and sealed to larger fluidic tubing using UV glue. The experimentation of the guidewire head actuation was conducted using a Fluigent Microfluidic Control System coupled with OxyGEN software (Fluigent, France). Air was pressurized through tubing and stainless-steel catheter couplers (20G, Instech, Plymouth Meeting, PA) at pressures increasing from 0 kPa to 600 kPa, holding at each pressure for 2 sec. ImageJ software (NIH) was used to quantify the actuation results.

Video was taken of these experiments with a Hayear Monocoluar Microscope and images were taken from these videos corresponding to the pressure inputs. Each image was uploaded into ImageJ to determine the radius of curvature and the XY locations of the middle and end of each guidewire head. The scale was set in mm based on the known capillary diameter of 360 μm, and the pixel-to-mm ratio was noted. Regions of Interest (ROIs) were then placed along the backbone of each segment of the actuator, with one point placed between each individual baffle. A circle was then manually fitted to the ROIs and was further adjusted to ensure accurate alignment along the curvature of the actuator. Once fit to the actuator, the radius of the circle was calculated, representing the radius of curvature of the bent actuator. Scalar (X-Y) coordinates were collected by pixel count from three critical points along the length of the actuator: (*i*) from the base of the baffle closest to the capillary, (*ii*) from the centroid of the connector between the two baffle segments, and (*iii*) from the outside tip of the baffle furthest from the capillary. By scaling the distance in pixels with the known pixel-to-mm ratio, the relative position of each of these critical points can be determined.

III. Results and Discussion

A. Fabrication via esDLW

CAM simulations and corresponding micrographs of the *es*DLW-printing process for both the symmetric and asymmetric guidewires are presented in Figure 2. Fabrication results of the two designs are shown in Figure 3. Both designs were manufactured with a 500 μm (*i.e.*, 1.5 Fr) outer diameter and a 2,500 μm height from the bottom of "bellow one" to the top of "bellow two" (not including the cylindrical base). Such aspect ratios are commonplace in catheter designs to match the dimensions of the vasculature through which it will

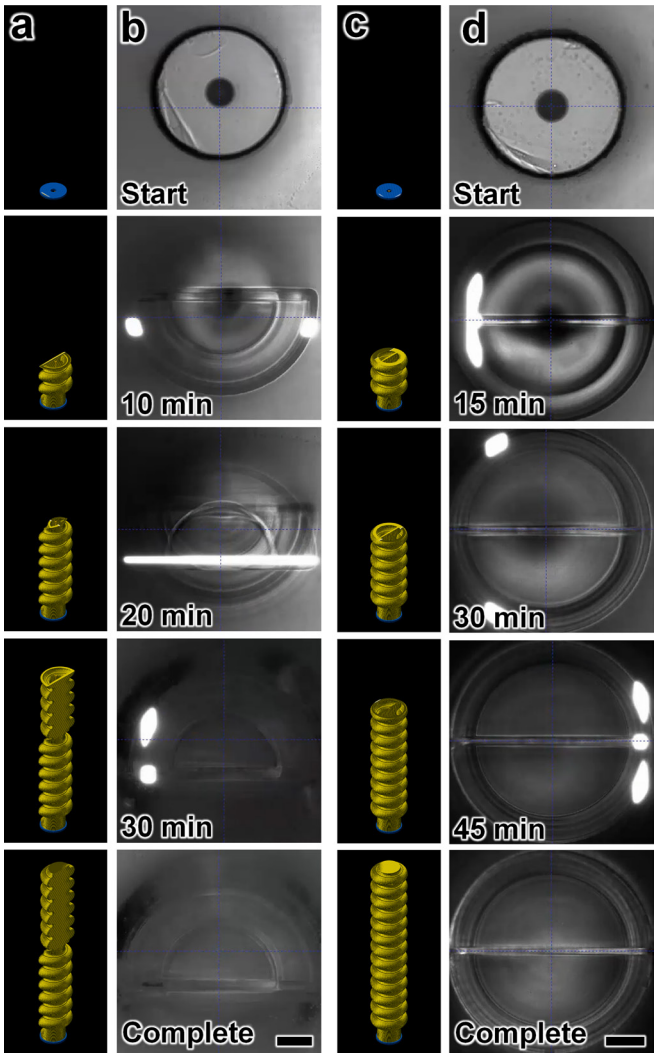

Figure 2. Fabrication results for the (a,b) asymmetric, and (c,d) symmetric designs. Sequential images of (a,c) computer-aided manufacturing (CAM) simulations, and (b,d) the corresponding *es*DLW 3D microprinting processes. Scale bars = 100 μm.

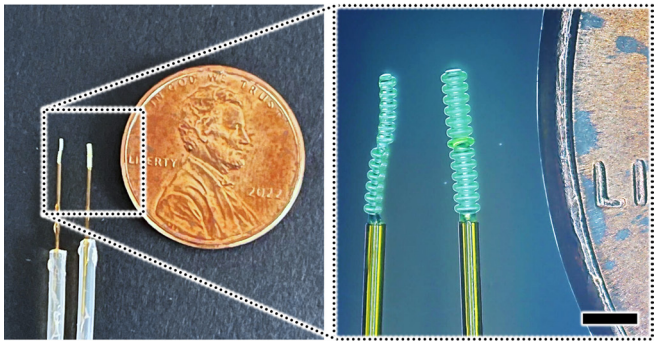

Figure 3. Fabrication results. The soft robotic guidewires printed atop and fluidically sealed to fused silica capillary tubes corresponding to (*left*) photograph and (*right*) brightfield microscope images. Scale bar = 1 mm.

ultimately travel [22], which was achievable in this work. Additionally, the 1.5 Fr outer diameter of the guidewires is a small enough diameter to traverse successfully through an infant's vasculature to the heart, such as in cases associated with PDA. A proof-of-concept example of the guidewire-catheter operation in which the catheter is sieved over the guidewire is presented in Figure 4.

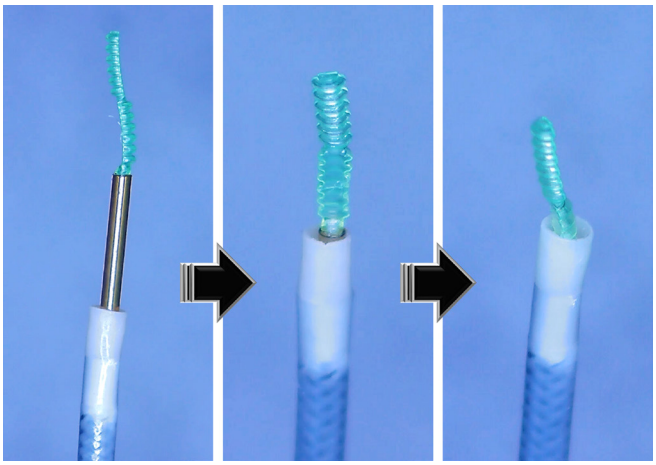

Figure 4. Successive images of a surgical catheter sliding over the 3D-microprinted guidewire system as a proof-of-concept demonstration of the guidewire-catheter systems eventual application.

B. Actuation Experimentation

To elucidate the actuation capabilities of the guidewire heads, we conducted testing in which an increasing pressure input was applied to each of the actuators. For the symmetric design, the radius of curvature decreased as the input pressure increased (Fig. 5a,b). We fitted this data to an exponential decrease with R^2 values of 0.94 and 0.85 for the bottom bellow and top bellow respectively (Fig. 5c). The symmetric design burst above 600 kPa and, thus, the maximum deformation was observed in the experiment. Bellow one was observed to have a larger change in radius of curvature from 0 to 550 kPa, transitioning from a radius of curvature of 21 mm to 2.2 mm in comparison to bellow two, which underwent a change in radius of 11 mm to 2.7 mm. This difference in behavior is likely due to the small channel connecting the two sets of bellows restricting flow in such a way that it causes a capacitive effect inside of bellow one, increasing its actuation. This capacitive effect can also be observed in the X-Y tracking of the middle and tip of the guidewire head (Fig. 7a). To achieve the required 'S' shape, the middle position should translate in one direction and the end position should translate in the other direction such that the end position is at the same horizontal position of the base. Because bellow one was actuating so much more than bellow two, this behavior was not observed. Instead, both the middle and the end point translated in the same direction as bellow one pressurized. Currently the two sections feature identical geometries, but future designs can account for the capacitive effect such that both bellows within the device actuate the same amount.

For the asymmetric design, a similar trend was seen in which the radius of curvature decreased as pressure increased (Fig. 6a,b), which fit to an exponential curve with R^2 values of 0.73 and 0.97 for the bottom bellow and top bellow, respectively (Fig. 6c). This design did not burst during testing in which the entire range of the available pressure was utilized, indicating that the asymmetric bellow was able to withstand higher pressures than the symmetric design. Both bellows in the asymmetric design resulted in a smaller radius of curvature

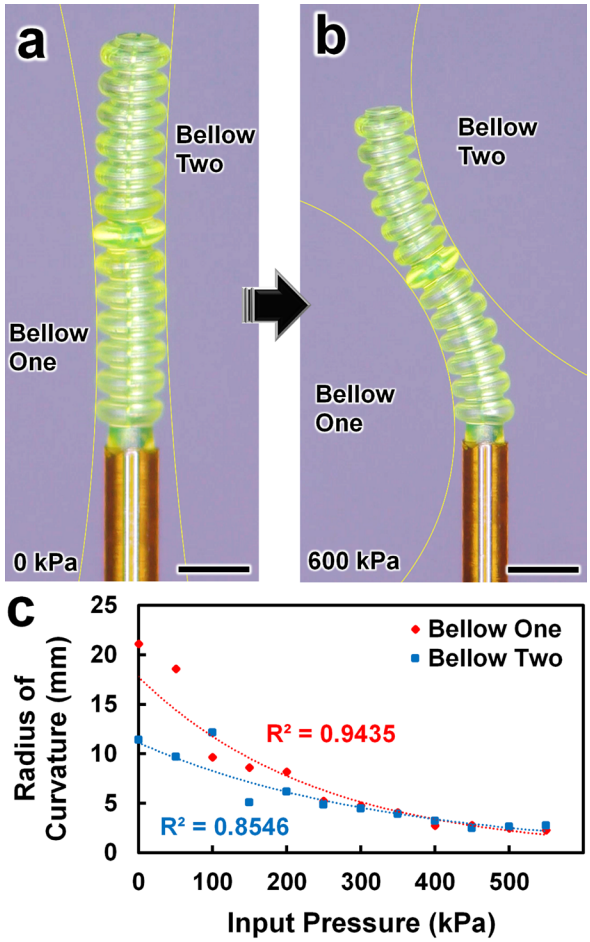

Figure 5. Experimental results for individual baffle curvature changes for the 3D-microprinted symmetric guidewire head under varying pneumatic loading conditions. (a,b) Brightfield micrograph of actuator curvature: (a) prior to pressure loading, and (b) under 600 kPa of applied pressure. Scale bar = 500 μm. (c) Quantified results for the radius of curvature *versus* applied pressure for each bellow.

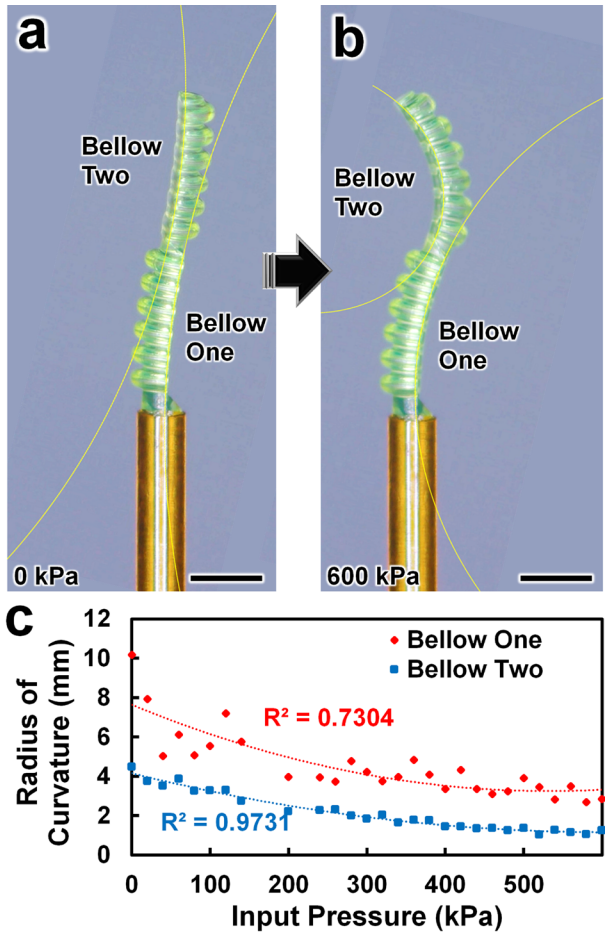

Figure 6. Experimental results for individual baffle curvature changes for the 3D-microprinted asymmetric guidewire head under varying pneumatic loading conditions. (a,b) Brightfield micrograph of actuator curvature: (a) prior to pressure loading, and (b) under 600 kPa of applied pressure. Scale bar = 500 μm. (c) Quantified results for the radius of curvature *versus* applied pressure for each bellow.

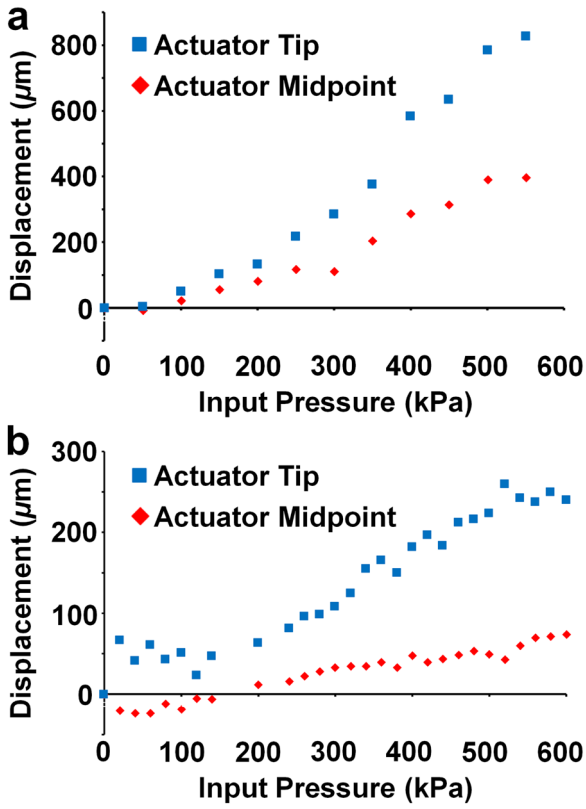

Figure 7. Displacement of the 3D-microprinted asymmetric guidewire tip and midpoint relative to their positions with zero pressure input for the: (a) symmetric design, and (b) asymmetric design.

at high pressure in comparison to the symmetric design at the same pressures; however, the bellows in the asymmetric design also began the experiment with a lower radius of curvature, likely due to deformation from shrinkage during post-processing. Throughout all the pressures tested, bellow two had a lower radius of curvature, implying increased actuation in comparison to bellow one, however, given that bellow two began testing with a smaller radius of curvature, this is likely also due to shrinkage during post processing. The X-Y tracking of the middle and end points in the asymmetric design are shown in Figure 7b. For this design, the two points moved in opposite directions to create the intended 'S' shape required for the application.

As an exploratory study, this work investigated the possibility of using *es*DLW to additively manufacture pneumatically actuated soft robotic guidewires for PDA intervention in infants. The surrogate fused silica capillary, which provided a suitable printing substrate, can be replaced with alternative medical tubing, such as that reported by Felix *et al.* [34]. To increase actuation curvature at lower (and safer) input pressures, the photoresin used in this study, IP-Dip2, can be replaced with a wide range of softer (and biocompatible) photosensitive materials, such as the commercially available polydimethylsiloxane (PDMS) photomaterial, IP-PDMS (Nanoscribe). In addition, higher numbers of bellows can be added to each actuation section dependent on patient specific anatomy, which would increase the tip deflections corresponding to each region.

IV. Conclusion

Endovascular interventions in the treatment of PDA in neonatal populations demand new guidewire-catheter systems that provide a means to overcome the pervasive navigational challenges associated with performing such procedures. In this work, we presented two novel 1.5 Fr, 2.5 mm-tall soft robotic guidewire designs—enabled by our *es*DLW 3D microprinting strategy—that are able to actuate to "S"-shaped configurations under applied fluidic pressures. The "S"-shaped architectures are particularly advantageous for PDA-associated guidewire navigation as they can mimic the shape of *in vivo* cardiac vessel pathways. In addition, because the design of the guidewire tip actuators can be modified as desired prior to 3D printing, the approach presented in this work could be leveraged for patient-specific soft robotic guidewires designed around unique cardiac anatomy on a case-by-case basis.

The ability to manage tight, opposing turns in small, delicate, and tortuous vessels has the potential to save time

and radiation exposure, while simultaneously mitigating risk by shortening procedure duration and increasing ease. We envision that such guidewires could also help bridge the differences in performance of junior *versus* senior operators in a field that is defined by vast anatomic variation with a wide spectrum of severity. Such capabilities would address unmet clinical needs for cardiac tools that allow for facile catheterization of tortuous, tiny arterial beds in young infants with unstable circulation. Thus, the presented approach and results serve as an important foundation for future efforts developing pediatric interventions in the treatment of PDA as well as for new classes of guidewire-catheters systems that could be applied to broad endovascular interventions that demand unique steering control capabilities at small scales.

ACKNOWLEDGMENT

The authors greatly appreciate the contributions of members of the Bioinspired Advanced Manufacturing (BAM) Laboratory and Terrapin Works staff at the University of Maryland, College Park. Any opinions, findings, and conclusions or recommendations expressed in this material are those of the authors and do not necessarily reflect the views of the National Science Foundation.

REFERENCES

[1] F.E.A. Udink ten Cate *et al.*, "Stenting the arterial duct in neonates and infants with congenital heart disease and duct-dependent pulmonary blood flow: A multicenter experience of an evolving therapy over 18 years," *Catheter. Cardiovasc. Interv.*, vol. 82, no. 3, pp. E233–E243, 2013.

[2] D. J. DiBardino *et al.* "A Review of Ductal Stenting in Hypoplastic Left Heart Syndrome: Bridge to Transplantation and Hybrid Stage I Palliation," *Pediatr. Cardiol.*, vol. 29, no. 2, pp. 251–257, 2008.

[3] E. A. Bacha *et al.*, "Single-ventricle palliation for high-risk neonates: The emergence of an alternative hybrid stage I strategy," *J. Thorac. Cardiovasc. Surg.*, vol. 131, no. 1, pp. 163-171.e2, 2006.

[4] E. Valencia *et al.*, "Transcatheter Ductal Stents Versus Surgical Systemic-Pulmonary Artery Shunts in Neonates With Congenital Heart Disease With Ductal-Dependent Pulmonary Blood Flow: Trends and Associated Outcomes From the Pediatric Health Information System Database," *J. Am. Heart Assoc.*, vol. 12, no. 17, p. e030528, 2023.

[5] A. C. Glatz *et al.*, "Comparison Between Patent Ductus Arteriosus Stent and Modified Blalock-Taussig Shunt as Palliation for Infants With Ductal-Dependent Pulmonary Blood Flow: Insights From the Congenital Catheterization Research Collaborative," *Circulation*, vol. 137, no. 6, pp. 589–601, 2018.

[6] H. M. Agha *et al.*, "Margin between success and failure of PDA stenting for duct-dependent pulmonary circulation," *PloS One*, vol. 17, no. 4, p. e0265031, 2022.

[7] A. M. Qureshi *et al.*, "Classification scheme for ductal morphology in cyanotic patients with ductal dependent pulmonary blood flow and association with outcomes of patent ductus arteriosus stenting," *Catheter. Cardiovasc. Interv. Off. J. Soc. Card. Angiogr. Interv.*, vol. 93, no. 5, pp. 933–943, 2019.

[8] M. Haga *et al*., "An Extremely Preterm Infant Born at 23 Weeks' Gestation With an Interrupted Aortic Arch Complex: A Case Report," *Cureus*, vol. 15, no. 7, p. e41389, 2023.

[9] L. Eilers and A. M. Qureshi, "Advances in Pediatric Ductal Intervention: an Open or Shut Case?," *Curr. Cardiol. Rep.*, vol. 22, no. 3, p. 14, 2020.

[10] V. N. Tolia *et al.*, "Low Rate of Spontaneous Closure in Premature Infants Discharged with a Patent Ductus Arteriosus: A Multicenter Prospective Study," *J. Pediatr.*, vol. 240, pp. 31-36.e2, 2022.

[11] T. Hundscheid *et al.*, "Understanding the pathobiology in patent ductus arteriosus in prematurity-beyond prostaglandins and oxygen," *Pediatr. Res.*, vol. 86, no. 1, pp. 28–38, Jul. 2019.

[12] S. K. Sathanandam *et al.*, "Amplatzer Piccolo Occluder clinical trial for percutaneous closure of the patent ductus arteriosus in patients ≥700 grams," *Catheter. Cardiovasc. Interv.*, vol. 96, no. 6, pp. 1266–1276, 2020.

[13] P. Morville and A. Akhavi, "Transcatheter closure of hemodynamic significant patent ductus arteriosus in 32 premature infants by amplatzer ductal occluder additional size-ADOIIAS," *Catheter. Cardiovasc. Interv.*, vol. 90, no. 4, pp. 612–617, 2017.

[14] B. H. Morray *et al.*, "3-year follow-up of a prospective, multicenter study of the Amplatzer Piccolo™ Occluder for transcatheter patent ductus arteriosus closure in children ≥ 700 grams," *J. Perinatol.*, vol. 43, no. 10, pp. 1238–1244, 2023.

[15] I. K. Yucel *et al.*, "A Challenging Interventional Procedure: Transcatheter Closure of Tubular Patent Ductus Arteriosus in Patients with Pulmonary Hypertension," *Pediatr. Cardiol.*, 2023.

[16] M. Wehner *et al.*, "An integrated design and fabrication strategy for entirely soft, autonomous robots," *Nature*, vol. 536, no. 7617, Art. no. 7617, 2016.

[17] P. E. Dupont *et al.*, "A decade retrospective of medical robotics research from 2010 to 2020," *Sci. Robot.*, vol. 6, no. 60, p. eabi8017, 2021.

[18] J. D. Greer, T. K. Morimoto, A. M. Okamura, and E. W. Hawkes, "A Soft, Steerable Continuum Robot That Grows via Tip Extension," *Soft Robot.*, vol. 6, no. 1, pp. 95–108, 2019.

[19] T. Gopesh *et al.*, "Soft robotic steerable microcatheter for the endovascular treatment of cerebral disorders," *Sci. Robot.*, vol. 6, no. 57, p. eabf0601, 2021.

[20] M. McCandless, A. Perry, N. DiFilippo, A. Carroll, E. Billatos, and S. Russo, "A Soft Robot for Peripheral Lung Cancer Diagnosis and Therapy," *Soft Robot.*, vol. 9, no. 4, pp. 754–766, 2022.

[21] G. Fagogenis *et al.*, "Autonomous robotic intracardiac catheter navigation using haptic vision," *Sci. Robot.*, vol. 4, no. 29, p. eaaw1977, 2019.

[22] J. Rogatinsky *et al.*, "A multifunctional soft robot for cardiac interventions," *Sci. Adv.*, vol. 9, no. 43, p. eadi5559, 2023.

[23] C. C. Nguyen *et al.*, "Development of a soft robotic catheter for vascular intervention surgery," *Sens. Actuators Phys.*, vol. 357, p. 114380, 2023.

[24] M. Li, R. Obregon, J. J. Heit, A. Norbash, E. W. Hawkes, and T. K. Morimoto, "VINE Catheter for Endovascular Surgery," *IEEE Trans. Med. Robot. Bionics*, vol. 3, no. 2, pp. 384–391, 2021.

[25] P. I. Baburova *et al.*, "Magnetic Soft Robot for Minimally Invasive Urethral Catheter Biofilm Eradication," *ACS Nano*, 2023,.

[26] G. Decroly, P. Lambert, and A. Delchambre, "A Soft Pneumatic Two-Degree-of-Freedom Actuator for Endoscopy," *Front. Robot. AI*, vol. 8, 2021.

[27] D. Van Lewen, T. Janke, H. Lee, R. Austin, E. Billatos, and S. Russo, "A Millimeter-Scale Soft Robot for Tissue Biopsy Procedures," *Adv. Intell. Syst.*, vol. 5, no. 5, p. 2200326, 2023.

[28] J. D. Hubbard *et al.*, "Fully 3D-printed soft robots with integrated fluidic circuitry," *Sci. Adv.*, vol. 7, no. 29, p. eabe5257, Jul. 2021.

[29] Y. Zhai *et al.*, "Desktop fabrication of monolithic soft robotic devices with embedded fluidic control circuits," *Sci. Robot.*, vol. 8, no. 79, p. eadg3792, 2023.

[30] A. T. Alsharhan, O. M. Young, X. Xu, A. J. Stair, and R. D. Sochol, "Integrated 3D printed microfluidic circuitry and soft microrobotic actuators *via in situ* direct laser writing," *J. Micromech. Microeng.*, vol. 31, no. 4, p. 044001, 2021.

[31] O. M. Young *et al.*, "3D Microprinting of Multi-Actuator Soft Robots onto 3D-Printed Microfluidic Devices *via Ex Situ* Direct Laser Writing," *20th Solid-State Sens. Actuators Microsyst. Workshop Hilton Head Isl. SC USA 2022*, pp. 332–335, 2022.

[32] R. Acevedo *et al.*, "3d Nanoprinted External Microfluidic Structures *via Ex Situ* Direct Laser Writing," in *2021 IEEE 34th International Conference on Micro Electro Mechanical Systems (MEMS)*, Jan. 2021.

[33] S. Sarker *et al.*, "3D-Printed Microinjection Needle Arrays via a Hybrid DLP-Direct Laser Writing Strategy," *Adv. Mater. Technol.*, vol. 8, no. 5, p. 2201641, 2023.

[34] B.M. Felix *et al.*, "Fabrication of Multilumen Microfluidic Tubing for *Ex Situ* Direct Laser Writing" in *2024 IEEE 37th International Conference on Micro Electro Mechanical Systems (MEMS)*, Austin, TX, USA, 2024.